BELLCOMM, INC.
955 L'ENFANT PLAZA NORTH, S.W. WASHINGTON, D.C. 20024

COVER SHEET FOR TECHNICAL MEMORANDUM

TITLE- Pinpoint Landing for a Lunar Payload Module

TM-68-2015-4

DATE- September 16, 1968

FILING CASE NO(S)- 340

AUTHOR(S)-H. W. Radin

FILING SUBJECT(S)- (ASSIGNED BY AUTHOR(S)-
Lunar Exploration
Lunar Payload Module
Pinpoint Landings
Terminal Guidance

ABSTRACT

In this memorandum we examine in detail the use of the Apollo sextant and LM Optical Rendezvous System (LORS) as aids for pinpoint landing an unmanned Lunar Payload Module (LPM). We conclude that for exploration sites equivalent to Apollo sites a 1σ accuracy of the order of 200 meters could be obtained, subject to feasibility of the operational technique.

Certain studies should be undertaken in the areas of sextant tracking simulation and guidance software to validate these results.

(NASA-CR-97695) PINPOINT LANDING FOR A LUNAR PAYLOAD MODULE (Bellcomm, Inc.) 32 p

N79-72522

00/19

Unclas
12672

SEE REVERSE SIDE FOR DISTRIBUTION LIST

DISTRIBUTION

COMPLETE MEMORANDUM TO

CORRESPONDENCE FILES:

OFFICIAL FILE COPY
plus one white copy for each additional case referenced

TECHNICAL LIBRARY (4)

NASA Headquarters

Messrs. R. J. Allenby/MAL
D. A. Beattie/MAL
G. F. Esenwein/MAL
T. A. Keegan/MA-2
D. R. Lord/MTD
B. Milwitzky/MAL
W. T. O'Bryant/MAL
L. R. Scherer/MAL

Manned Spacecraft Center

Messrs. S. M. Andrich/ET
H. D. Beck/FM5
R. L. Bond/PD8
J. H. Boynton/FM13
D. C. Cheatham/EG
W. N. Hess/TA
J. D. Hodge/HA
M. D. Jenness/FM5
M. Kayton/EG
J. Loftus/HA
C. E. Manry/EG26
J. P. Mayer/FM
O. E. Maynard/PD
A. J. Meyer/HA
W. J. North/CF
J. Sasser/TH3
R. T. Savely/FM4
H. H. Schmitt/CB
G. Xenakis/EG

Marshall Space Flight Center

Messrs. J. A. Belew/R-AS-A
F. L. Williams/R-AS-DIR

Massachusetts Institute of Technology

Messrs. I. Johnson
G. M. Levine

Bellcomm, Inc.

Messrs. F. G. Allen
G. M. Anderson
D. R. Anselmo
D. J. Belz
G. L. Bush
A. P. Boysen, Jr.
J. O. Cappellari, Jr.
D. A. Chisholm
D. A. Corey
T. H. Crowe
C. L. Davis
D. A. DeGraaf
J. P. Downs
D. R. Hagner
P. L. Havenstein
F. Heap
W. G. Heffron
A. Heiber
N. W. Hinners
B. T. Howard
D. B. James
A. N. Kontaratos
J. Kranton
M. Liwshitz
H. S. London
R. K. McFarland
J. L. Marshall
K. E. Martersteck
J. Z. Menard
A. C. Merritt
V. S. Mummert
B. G. Niedfelt
G. T. Orrok
V. L. Osborne
P. E. Reynolds
F. N. Schmidt
R. V. Sperry
W. Strack
W. B. Thompson
J. W. Timko

DISTRIBUTION

COMPLETE MEMORANDUM TO

R. Vernon
J. E. Volonte
R. L. Wagner
J. E. Waldo
All Members Department 2015
Department 1024 Files

COVER SHEET ONLY TO

Bellcomm, Inc.

Mr. I. M. Ross

BELLCOMM, INC.
955 L'ENFANT PLAZA NORTH, S.W. WASHINGTON, D. C. 20024

SUBJECT: Pinpoint Landing for a Lunar Payload Module - Case 340

DATE: September 16, 1968

FROM: H. W. Radin

TM-68-2015-4

TECHNICAL MEMORANDUM

1.0 INTRODUCTION

In the later stages of lunar exploration, it will be necessary to land large amounts of astronaut support equipment on the Moon, close to an exploration site.* Since the prime prospect for a supply vehicle is an unmanned LM, or Lunar Payload Module (LPM), and since the current capability of the LM for accurate landings depends on LM astronaut participation, this study was undertaken to examine alternate techniques for pinpoint landing.

Several techniques have been suggested; this memorandum discusses the joint use of the CSM sextant (SXT) and the LM Optical Rendezvous System (LORS)** for descent guidance. For the present study, the CSM will be assumed to be manned, and the landing site to have no artificial markers to aid in descent guidance.

2.0 GENERAL DESCRIPTION OF THE LORS/SXT METHOD

This approach to terminal guidance takes advantage of the astronaut's abilities in pattern recognition: the CSM astronaut will search the terrain beneath him, compare it with lunar surface charts, and identify the landing site. He will

---

*Hinners, N. W., D. B. James, and F. N. Schmidt, A Lunar Exploration Program, TM-68-1012-1, January 5, 1968.

**The LORS is an automatic optical tracking device, which can automatically acquire a flashing CSM beacon at a range of 400 nautical miles (740 km) within a field of view of 0.6 degrees (10 mr), and track it with an accuracy of 0.15 mr. The output of the LORS goes directly to the LPM computer. (The LORS has been developed as a backup to the LM rendezvous radar.)

then train the star line of sight (SLOS)* of the CSM sextant on the landing site and press the mark button, transferring the azimuth and elevation information to the CSM computer; this information will then be telemetered to the LPM computer. This is the unit vector $\bar{v}_{CS}$ from the CSM to the landing site (see Figure 1).

Simultaneously, the LORS will automatically track the CSM from the LPM, aided by a flashing light beacon on the CSM, and provide azimuth and elevation data to the LPM computer. This is the unit vector $\bar{v}_{LC}$ from the LPM to the CSM.

The magnitudes of these two vectors will be obtained approximately from the known heights of the CSM and LPM above a smooth Moon, as determined from the landing radar and MSFN tracking.** The LPM computer will then calculate an update on the vector $\bar{V}_{LS}$ from the LPM to the landing site by adding the above two vectors.

3.0 DESCRIPTION AND ANALYSIS

3.1 Acquisition

The CSM astronaut must acquire the landing site visually with the SLOS at some time prior to a few minutes before LPM touchdown. For an 80 nautical mile CSM orbit, the landing site is first visible at the horizon about 7-1/2 minutes before it is directly beneath the CSM; thus the acquisition process cannot begin until

---

*The landmark line of sight of the sextant is not used. The sextant cannot be used in its normal two-axis mode for this purpose, since the computer is automatically given only the vector directions of the optical axes of the two lines of sight. This can be seen by imagining that the two sextant axes have been pointed at the LPM and the landing site, with superposition obtained at the center of the field. If now the two axes are moved slightly, but not relative to one another, the images will remain superimposed but at a point off the center of the field. Thus the vector directions of the optical axes given to the computer will not represent the directions to the LPM and landing site.

It is probably not realistic to require the astronaut to perform the superposition only at the center of the field.

**An alternative is combining data from the landing radar, VHF ranging device, and LORS/SXT tracking to give a more precise estimate of Δh_C and Δh_L.

then. About six minutes elapses before the landing site is 45° ahead of the local vertical at the CSM (45° declination); this period may be used for acquisition. At the end of the acquisition period the slant range to the landing site is 113 nautical miles, or 210 kilometers; the 5 x 7 km landing ellipse subtends an angle of about 1.4 degrees, just about filling the 1.8 degree field of view of the sextant.

Acquisition of the CSM by the LORS is an automatic search process, within a 10 milliradian field of view; this field should be easily sufficient. The relative location of the CSM is known precisely until separation, and thereafter to an accuracy determined only by navigational uncertainties and IMU misalignments in the CSM and LPM. Except for the short separation and Hohmann transfer burn periods, the LPM is in free fall until the start of powered descent. Thus, acquisition of the CSM may be made at any time by pointing the LORS in the anticipated direction within 10 mr (0.6 degrees). The best way would be to acquire before or immediately after separation, and search only to recover from accidental loss of lock.

3.2 Tracking

The CSM astronaut is required only to keep the SLOS of the sextant pointed at the landing site, and to press the mark button whenever it is accurately centered. Since this must be done in the face of very high elevation angle rates (see Appendix A and Figure 2), one might question his ability even to keep the landing site in the field of view--related simulation evidence indicates, however, that this is likely to be a reasonable task.* The problem is quite similar to lunar landmark tracking, which is currently a test objective on Apollo Missions F and G.

Should later evidence disprove this conclusion, it is alternatively suggested that the CSM computer control the spacecraft attitude in accordance with its prediction of the landing site elevation, thus keeping the SLOS pointed approximately at the landing site. When the astronaut is ready to center the SLOS he will take over control of the SLOS from the computer, <u>but the CSM attitude rate that the computer had commanded will remain</u>--thus the astronaut begins with a stable image,** and need introduce only differential attitude rates.

---

*Ivan Johnson, MIT Instrumentation Laboratory, private communication.

**This type of software might also be useful for CSM orbital photography, perhaps on the same mission.

As an example, allow the computer to point the SLOS at the landing site initially, and to increment the CSM attitude rate by 0.1 degrees per second whenever the landing site elevation rate reaches this value. Then the maximum attitude rate apparent to the astronaut will be 0.1 degrees per second. Figure 3 shows the resulting apparent attitude rate; it can be seen that the time intervals during which the astronaut has control of the SLOS decrease as the CSM approaches the landing site. The smallest interval, commencing about 60 seconds before the CSM passes over the landing site, is about 25 seconds.

An interval of nearly 100 seconds occurs near the time the CSM passes over the LPM and the landing site (about 170 seconds before LPM touchdown); this is the most critical time, when the measurement accuracy is best (see Section 3.3).

3.3 Accuracy

The principal contributor to error in this technique is inaccurate knowledge of the height of the LPM above the landing site (see Appendix B). The LPM or CSM height uncertainties have three components:

1. The uncertainty in the distance of the orbiting CSM/LPM combination or the descending LPM from the center of mass of the Moon, as obtained from MSFN tracking.

2. The uncertainty in the distance of the surface of a mean, smooth, aspherical Moon from its center of mass.

3. Topographic irregularities superimposed on the mean surface.

The 1σ value of LPM height uncertainty, incorporating components 1 and 2, is currently thought to be about 350 meters, with the CSM height uncertainty having a comparable value.* For an Apollo-equivalent site, the contribution due to topographic uncertainties

---

*MSC Memorandum 68-FM46-109, W. R. Wollenhaupt, March 27, 1968. (Δh_C is given as 332 m.); MIT Instrumentation Laboratory Memorandum E-1982, LEM PNGCS and Landing Radar Operations during the Powered Landing Maneuver, B. Kriegsman and N. Sears, August 1966. (Δh_L is given as 1139 ft.)

may be assumed to be about an equal amount (the height error 10 km uprange of the landing site--high gate--due to a 2° surface slope is just 350 meters). An rss addition of these two 350 m components yields approximately a 500 m composite 1σ error in CSM and LPM height; the resulting error in downrange distance measurement is shown in Figure 4. (When the landing radar comes on, it will reduce the LPM height error due to MSFN tracking to some smaller value. The component due to lunar surface elevation errors relative to the landing site will remain.)

The 1σ downrange residual error which cannot be removed by LORS/SXT tracking has a value of about 170 meters,* assuming the last measurement** is taken where the $(\Delta D)_{rss}$ curve is a minimum, near high gate. Assuming errors of 1 km in h_L and h_C, the corresponding value of $(\Delta D)_{rss}$ is about 180 meters (see Figure 5); a 2 km error in height leads to about a 215 meter downrange error (Figure 6).

The companion Figures 7, 8, and 9, show the four components of the downrange error, and make clear the dominance of the $\Delta h_L \tan \xi$ component (ξ is the angle to the LPM from the CSM local vertical); this portion goes to zero when the CSM is directly over the LPM, which occurs approximately at high gate for the standard Apollo trajectory used. The crossrange error is shown in Figure 10; Figures 11 and 12 describe the trajectory.

Thus the LORS/SXT technique is quite accurate for terrain which is itself accurately described (downrange errors are due principally to errors in the knowledge of relative surface heights).

4.0 IMPACT ON APOLLO DESIGN

4.1 Hardware

There are two principal hardware requirements for the LORS/SXT system: a telemetry link and the LORS itself. A telemetry link is required in order to communicate the results of an SXT update of the landing site to the LPM computer, which will perform the final update computations. A command link is already

---

*As with any such scheme, the physical dimensions of the surface object tracked (crater, etc.) will also affect the accuracy. For example, the center of a 10 km crater cannot be found to 1 meter accuracy.

**We assume a series of measurements, having steadily improving accuracy, with the last measurement taken where the error curve is a minimum. Gross errors may thus be corrected early where the fuel cost is lower.

planned for the LM-ATM, and could be adapted to a lunar LPM, but the useful data transfer rate is too low due to extensive checking and verifying procedures. Modification of these procedures could probably reduce the transmission time for a state vector update from the current 14 seconds (approximately) to about 2 or 3 seconds.

The LORS has been developed as a backup to the LM rendezvous radar, although a flight model is not presently available.

4.2 Software

Software modifications are needed for two purposes: to permit the CSM computer to assist the astronaut in attitude control, and to permit the LPM computer to absorb telemetered data from the CSM. The former is a relatively minor change, while the latter may be substantial--some study of this question is essential.

The question of update weighting functions should be reexamined for this update technique, in view of the steadily improving accuracy as a function of T_{go} and the opportunity to mop up control errors.

4.3 Astronaut Training and Simulation

While the tasks required of the CSM astronaut(s) are not excessive, the angular rate of tracking for the mode without computer assistance is quite high. An early simulation of this problem should be made to evaluate the time constraints and to determine the astronaut's tracking abilities at these rates. Such a simulation would also be a useful preliminary to the lunar landmark tracking test objectives of Apollo Missions F and G.

5.0 CONCLUSIONS AND RECOMMENDATIONS

We have shown that the joint use of the LORS and the CSM sextant may permit an LPM landing accuracy of the order of 200 meters (1σ), under reasonable assumptions concerning the knowledge of lunar surface elevations. These assumptions are met, for example, for all Apollo sites, and for some Apollo-equivalent exploration sites.

For many scientific exploration sites, the problem is tougher for two reasons: the terrain itself is often more topographically violent, and our photography of the sites is more limited in its quantitative accuracy. The result is a more limited potential for landing accuracy, and a need for additional fuel margins to permit LPM descent from the minimum safe height. Work on this technique for the science sites is continuing.

It should be noted that, although a typical Apollo descent profile was used for convenience, there is no particular reason to retain this constraint for an LPM mission. For example, the visibility phase could be eliminated, the flight path angle increased, and the lighting conditions modified. A substantial fuel saving would probably result.

With regard to the Apollo candidate sites, certain points should be studied in order to validate this technique:

1. The ability of a CSM astronaut to perform the requisite tracking tasks with the sextant at the high angular rates involved. Present indications are, from related simulations, that he can do so. In particular, a specific simulation should be performed.

2. The extent of the software changes necessary to utilize the LORS/SXT updates in the CSM or LPM guidance computers (including time synchronization of the LORS and SXT measurements), along with a consideration of the weighting functions to be used. A more detailed error analysis should also be performed.

3. The specifics of the logic changes needed to speed up the transmission of telemetry data from the CSM to the LPM (telemetry hardware is currently planned for the LM-ATM).

In summary, the use of the LORS/SXT combination may permit a substantial improvement in the landing accuracy of an LPM (actually the present quoted 5 x 7 km error ellipse of the LM).

6.0 ACKNOWLEDGMENTS

My particular thanks go to I. Silberstein for many helpful discussions on this and related problems. F. Heap and V. L. Osborne provided an essential computer printout on very short notice, and I. L. Johnson of the MIT Instrumentation Laboratory was most generous with his time in discussions of the proposal.

HW Radin

2015-HWR-acm H. W. Radin

Attachments
- References
- Figures 1 - 12
- Appendix A
- Appendix B
- Appendix C

REFERENCES

1. Hinners, N. W., D. B. James, and F. N. Schmidt, A Lunar Exploration Program, TM-68-1012-1, January 5, 1968

2. Wollenhaupt, W. R., MSC Memorandum 68-FM46-109, March 27, 1968.

3. Kriegsman, B., and N. Sears, MIT Instrumentation Laboratory Memorandum E-1982, LEM PNGCS and Landing Radar Operations during the Powered Landing Maneuver, August 1966.

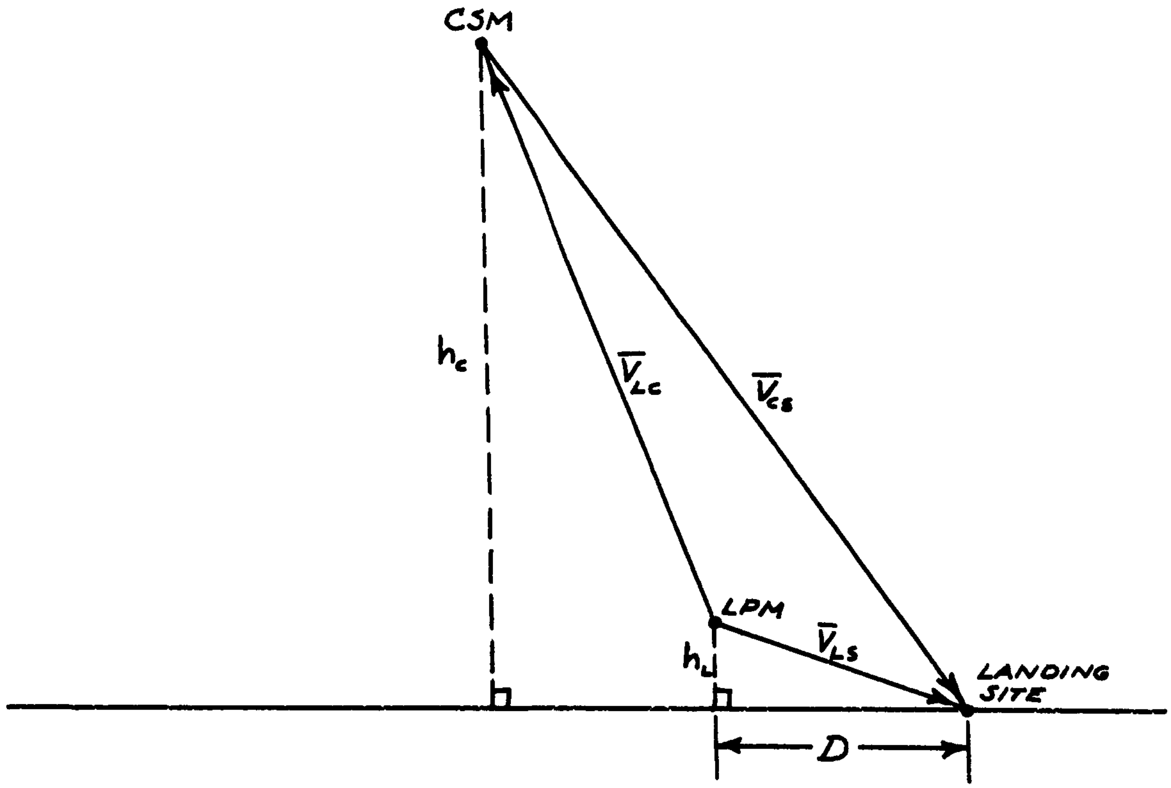

$$\overline{V}_{LS} = \overline{V}_{LC} + \overline{V}_{CS}$$

FIGURE 1. LORS/SEXTANT GEOMETRY

LANDING SITE TRACKING RATE

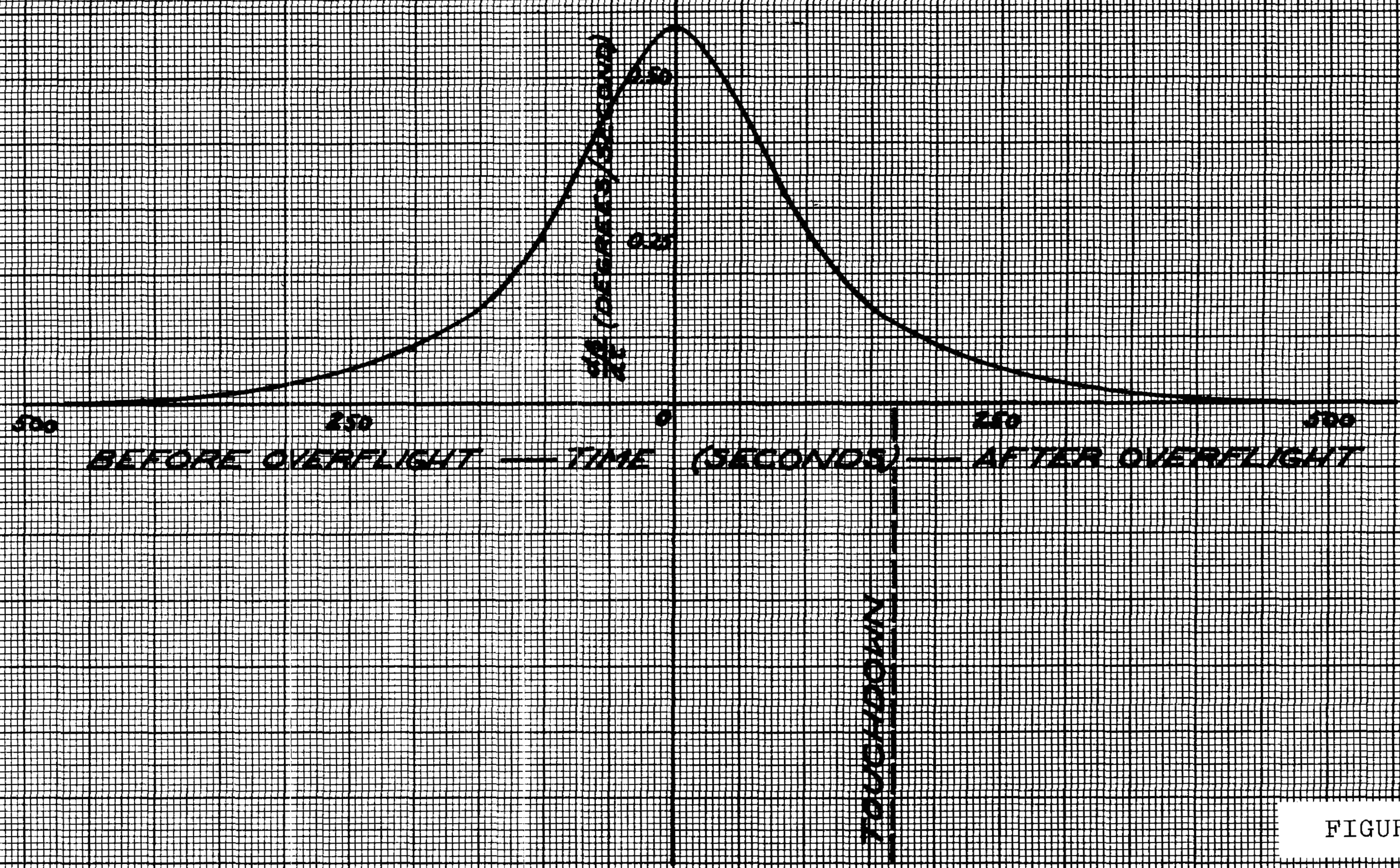

FIGURE 2

HARADIN
6-19-62

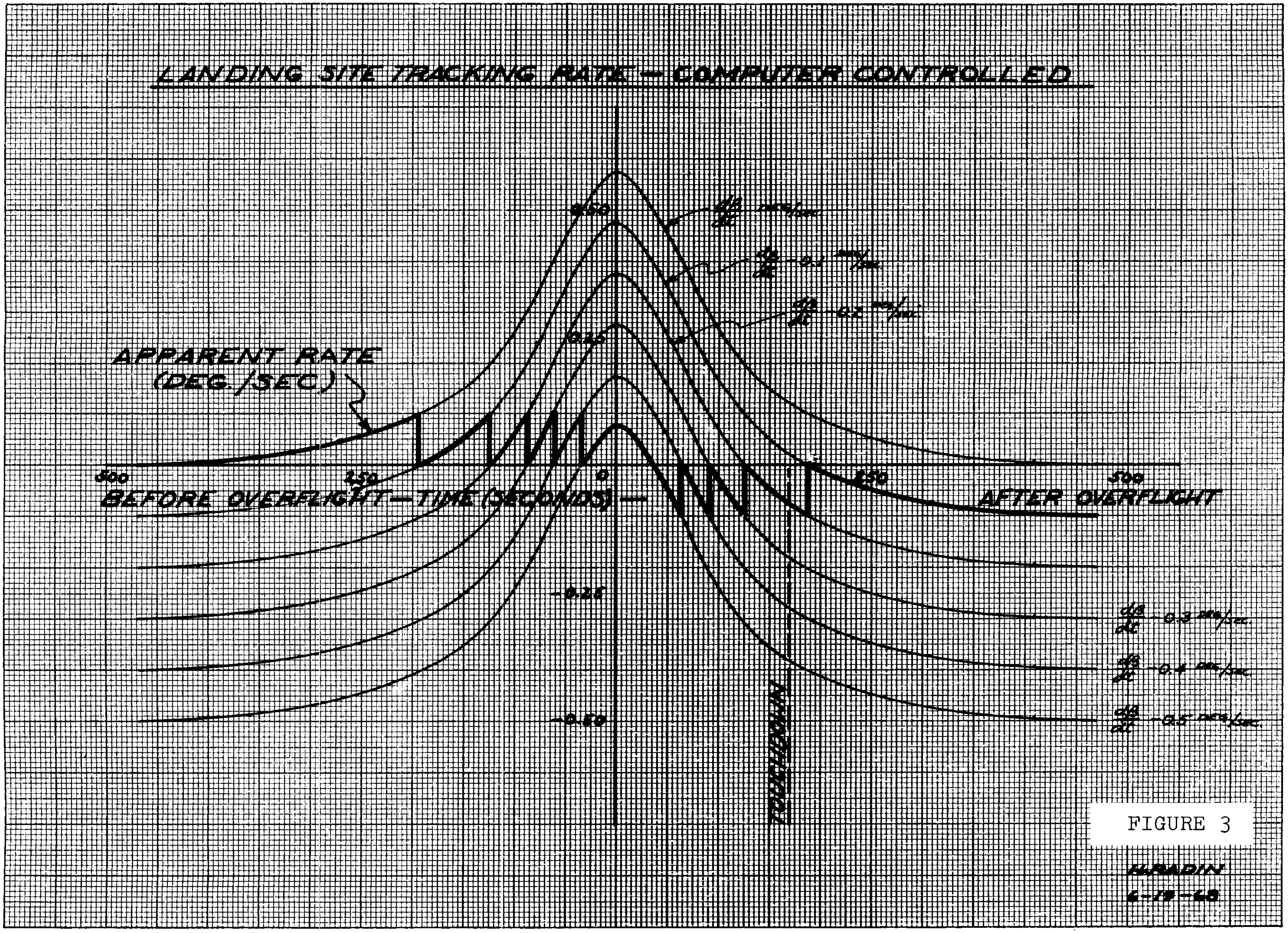
LANDING SITE TRACKING RATE — COMPUTER CONTROLLED
APPARENT RATE
(DEG./SEC.)
0.50
0.25
0
-0.25
-0.50
500
250
0
250
500
BEFORE OVERFLIGHT — TIME (SECONDS) — AFTER OVERFLIGHT
TOUCHDOWN
dθ/dt DEG/SEC
dθ/dt - 0.1 DEG/SEC
dθ/dt - 0.2 DEG/SEC
dθ/dt - 0.3 DEG/SEC
dθ/dt - 0.4 DEG/SEC
dθ/dt - 0.5 DEG/SEC
H. RADIN
6-19-68

FIGURE 3

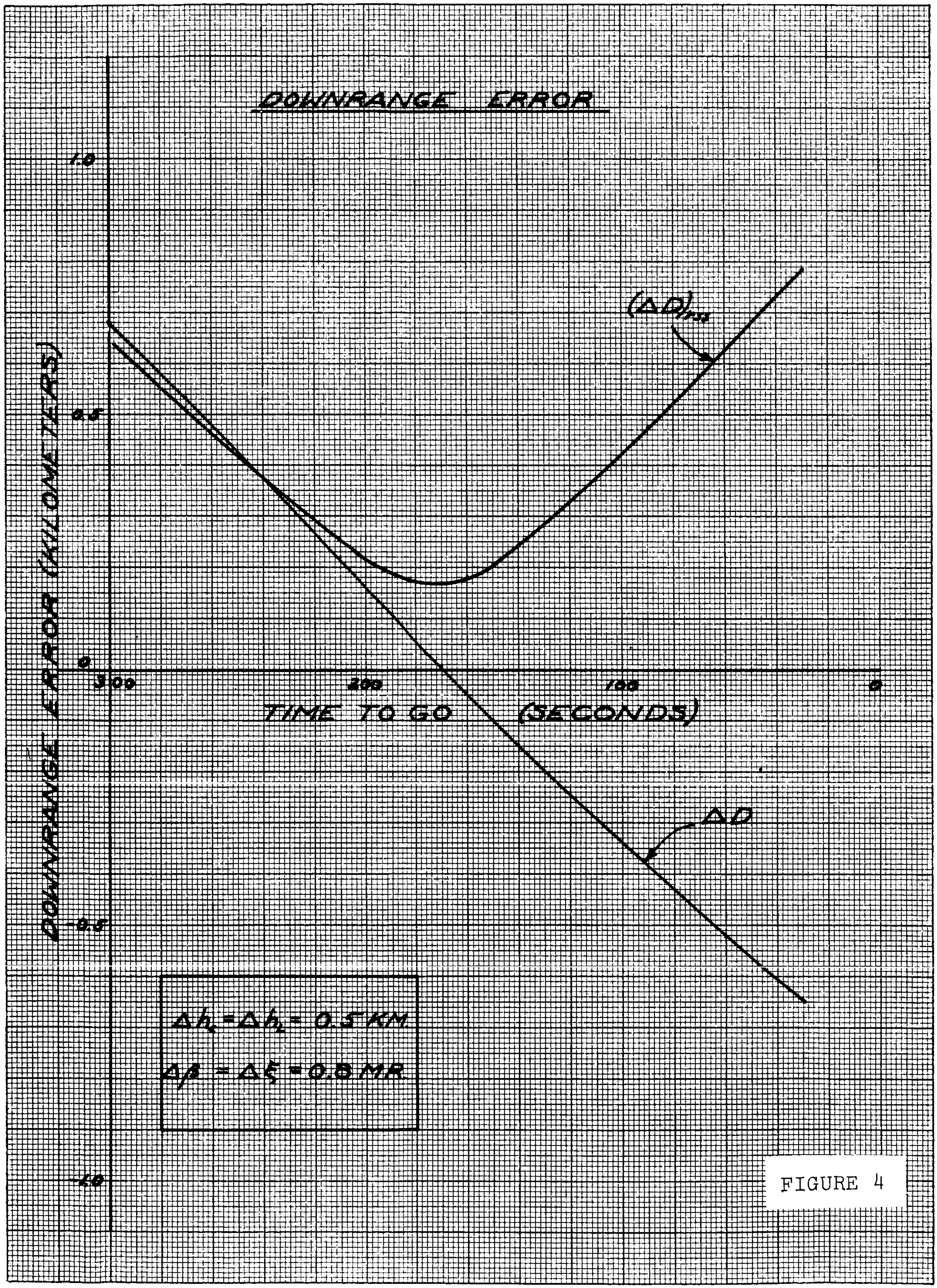
DOWNRANGE ERROR
DOWNRANGE ERROR (KILOMETERS)
TIME TO GO (SECONDS)
1.0
0.5
0
-0.5
-1.0
300
200
100
0
$(\Delta D)_{rss}$
ΔD
$\Delta h_1 = \Delta h_2 = 0.5$ KM
$\Delta\beta = \Delta\xi = 0.8$ MR

FIGURE 4

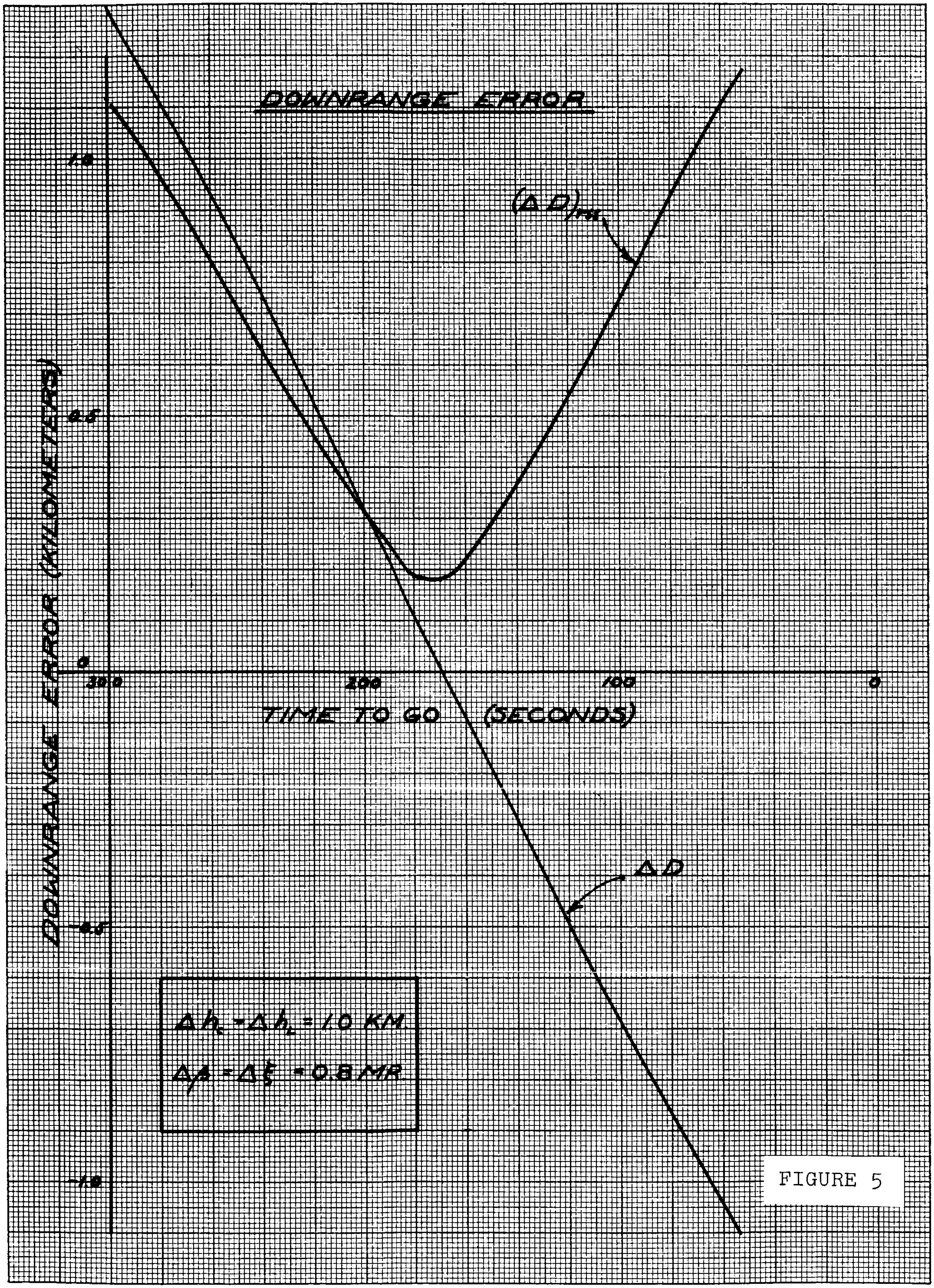
DOWNRANGE ERROR
DOWNRANGE ERROR (KILOMETERS)
TIME TO GO (SECONDS)
1.0
0.5
0
-0.5
-1.0
300
200
100
0
(ΔD)m
ΔD
Δh_c = Δh_L = 1.0 KM
Δβ = Δξ = 0.8 MR

FIGURE 5

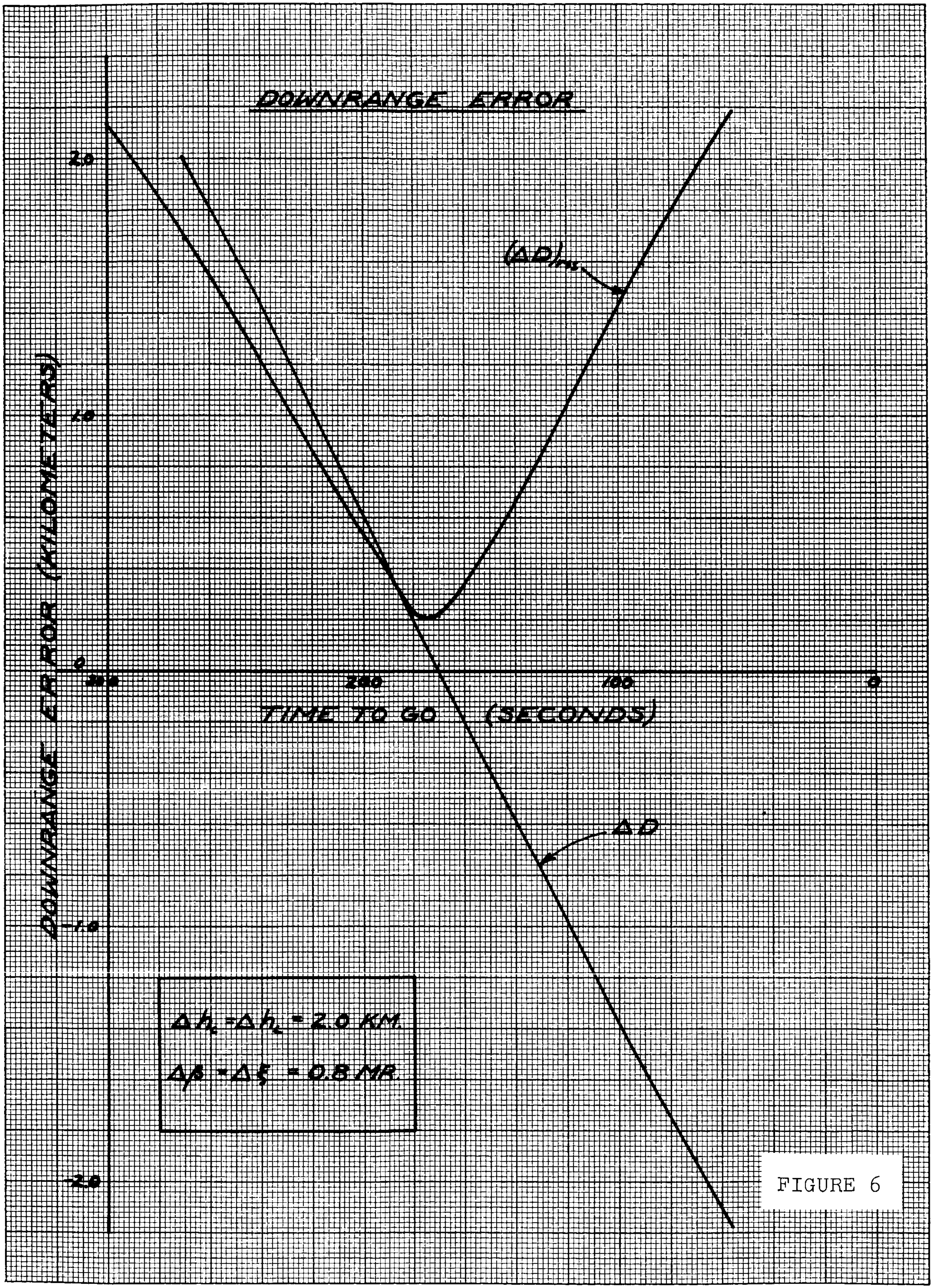
DOWNRANGE ERROR
DOWNRANGE ERROR (KILOMETERS)
TIME TO GO (SECONDS)
2.0
1.0
0
-1.0
-2.0
200
100
0
$(\Delta D)_{RS}$
ΔD
$\Delta h_c = \Delta h_L = 2.0$ KM.
$\Delta\beta = \Delta\xi = 0.8$ MR.

FIGURE 6

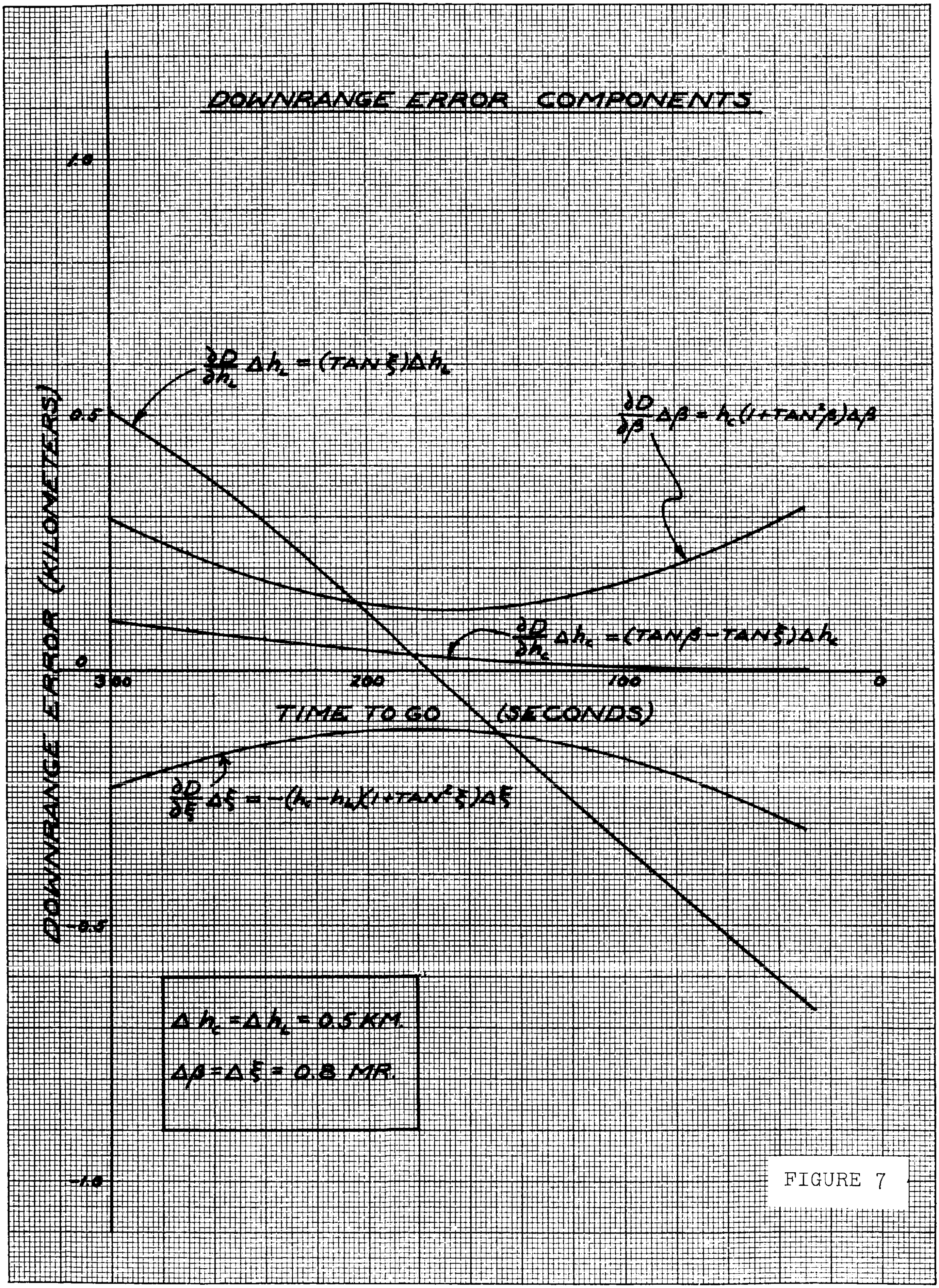
DOWNRANGE ERROR COMPONENTS
DOWNRANGE ERROR (KILOMETERS)
1.0
0.5
0
-0.5
-1.0
300
200
100
0
TIME TO GO (SECONDS)
$\frac{\partial D}{\partial h_L}\Delta h_L = (TAN\,\xi)\Delta h_L$
$\frac{\partial D}{\partial \beta}\Delta\beta = h_c(1+TAN^2\beta)\Delta\beta$
$\frac{\partial D}{\partial h_c}\Delta h_c = (TAN\,\beta - TAN\,\xi)\Delta h_c$
$\frac{\partial D}{\partial \xi}\Delta\xi = -(h_c - h_L)(1+TAN^2\xi)\Delta\xi$
$\Delta h_c = \Delta h_L = 0.5$ KM.
$\Delta\beta = \Delta\xi = 0.8$ MR.
FIGURE 7

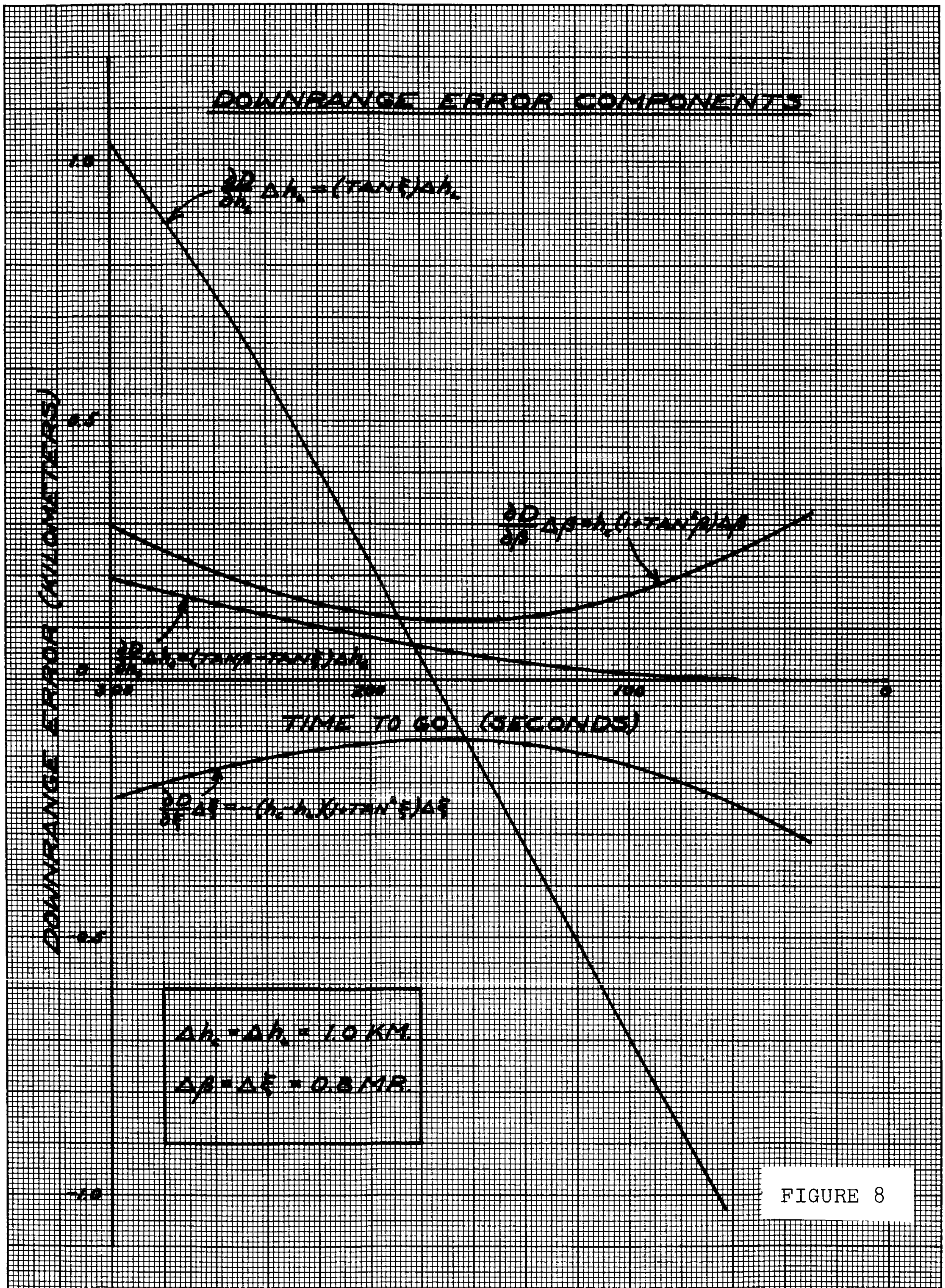
DOWNRANGE ERROR COMPONENTS
DOWNRANGE ERROR (KILOMETERS)
1.0
0.5
0
-0.5
-1.0
300
200
100
0
TIME TO GO (SECONDS)
$\frac{\partial D}{\partial h_c}\Delta h_c = (TAN\,\xi)\Delta h_c$
$\frac{\partial D}{\partial \beta}\Delta\beta = h_c(1+TAN^2\beta)\Delta\beta$
$\frac{\partial D}{\partial h_o}\Delta h_o = (TAN\beta - TAN\xi)\Delta h_o$
$\frac{\partial D}{\partial \xi}\Delta\xi = -(h_c - h_o)(1+TAN^2\xi)\Delta\xi$
$\Delta h_c = \Delta h_o = 1.0$ KM.
$\Delta\beta = \Delta\xi = 0.5$ MR.

FIGURE 8

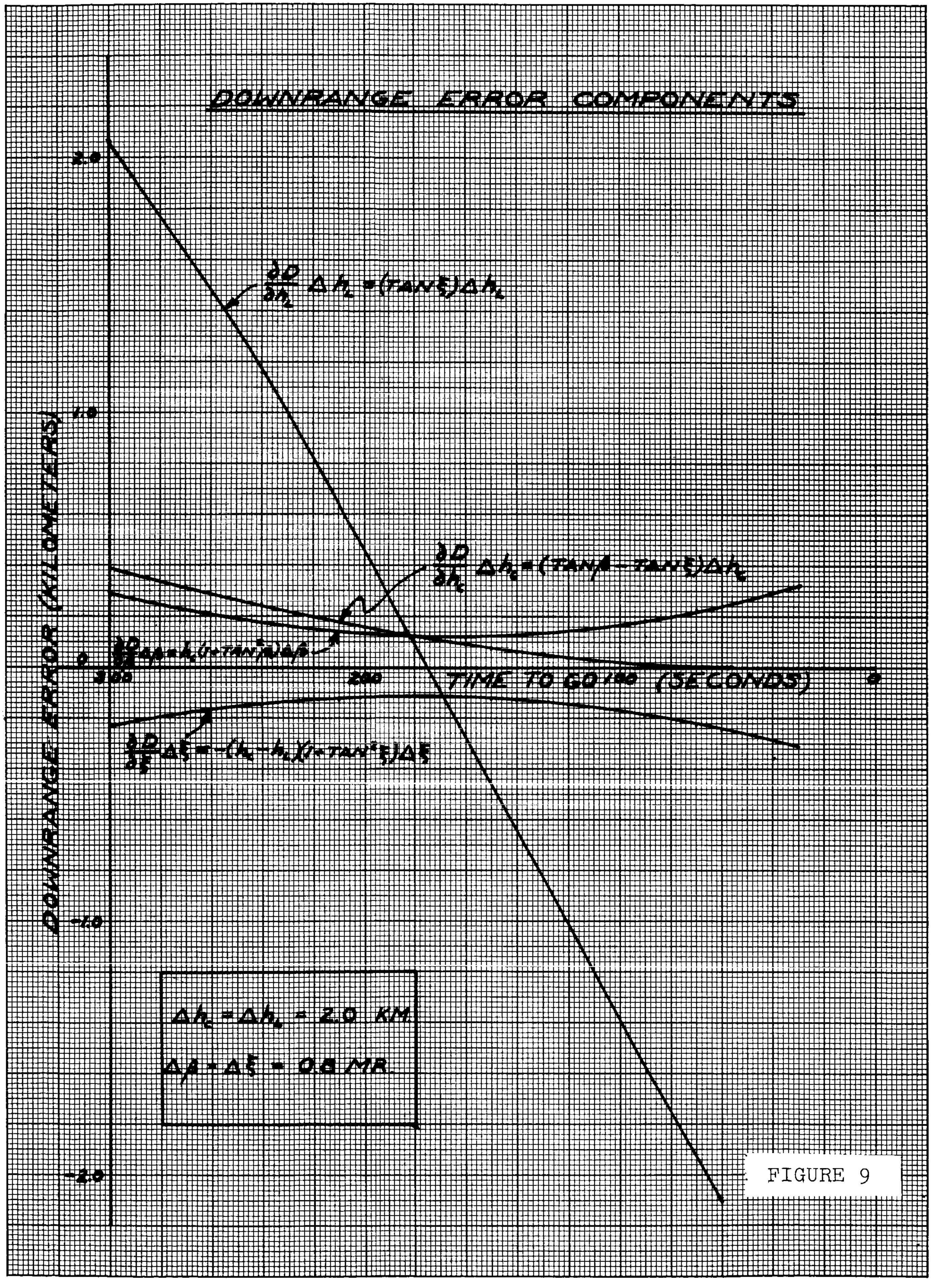

DOWNRANGE ERROR COMPONENTS
DOWNRANGE ERROR (KILOMETERS)
2.0
1.0
0
-1.0
-2.0
300
200
TIME TO GO 100 (SECONDS)
0
$\frac{\partial D}{\partial h_L} \Delta h_L = (TAN\,\xi)\Delta h_L$
$\frac{\partial D}{\partial h_c} \Delta h_c = (TAN\,\beta - TAN\,\xi)\Delta h_c$
$\frac{\partial D}{\partial \beta} \Delta\beta = h_c(1 + TAN^2\beta)\Delta\beta$
$\frac{\partial D}{\partial \xi} \Delta\xi = -(h_c - h_L)(1 + TAN^2\xi)\Delta\xi$
$\Delta h_c = \Delta h_L = 2.0$ KM.
$\Delta\beta = \Delta\xi = 0.8$ MR.

FIGURE 9

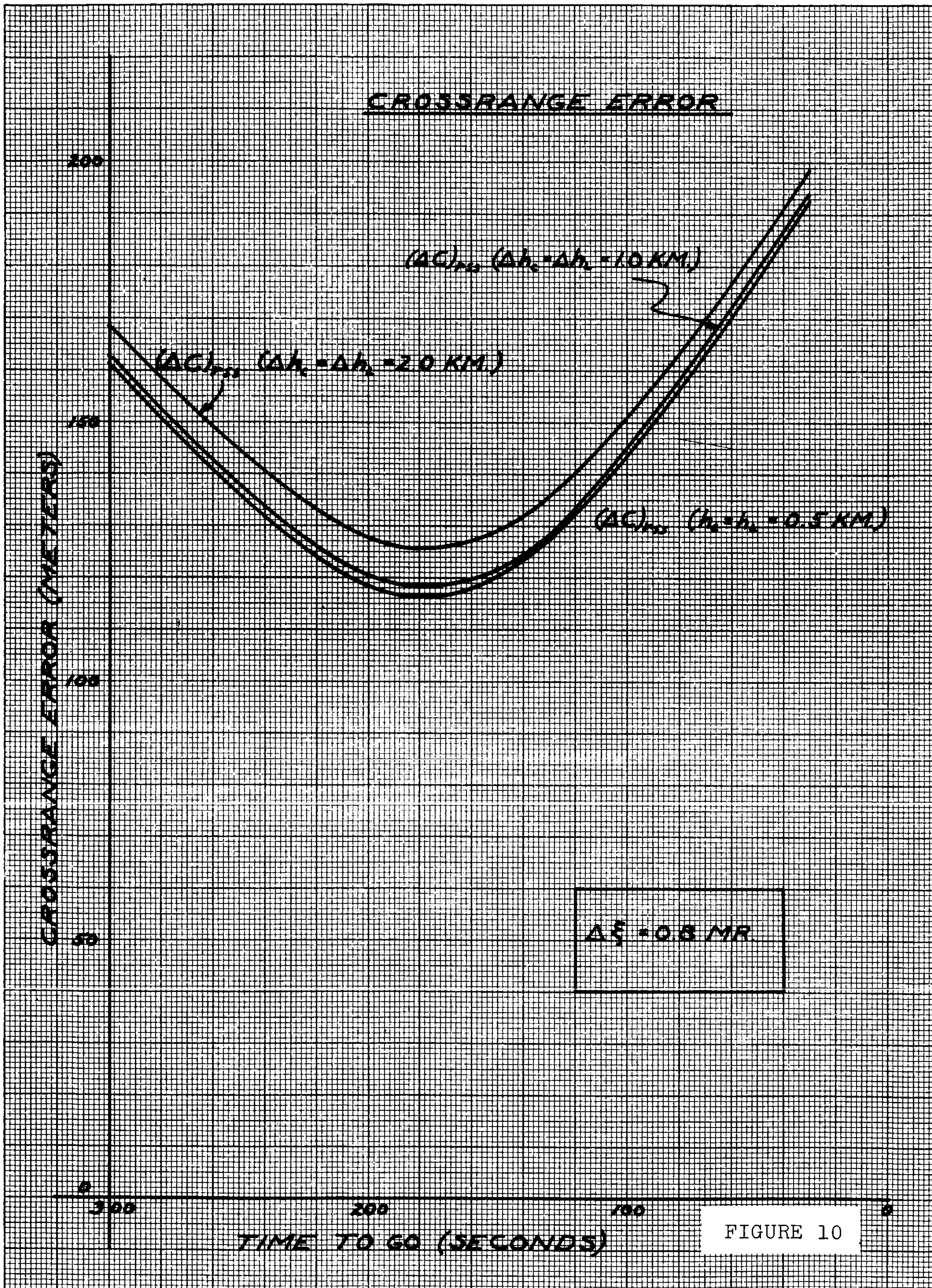

CROSSRANGE ERROR
$(\Delta C)_{rss}$ $(\Delta h_c = \Delta h_t = 1.0$ KM.)
$(\Delta C)_{rss}$ $(\Delta h_c = \Delta h_t = 2.0$ KM.)
$(\Delta C)_{rss}$ $(h_c = h_t = 0.5$ KM.)
$\Delta \xi = 0.8$ MR
200
150
100
50
0
300
200
100
0
CROSSRANGE ERROR (METERS)
TIME TO GO (SECONDS)

FIGURE 10

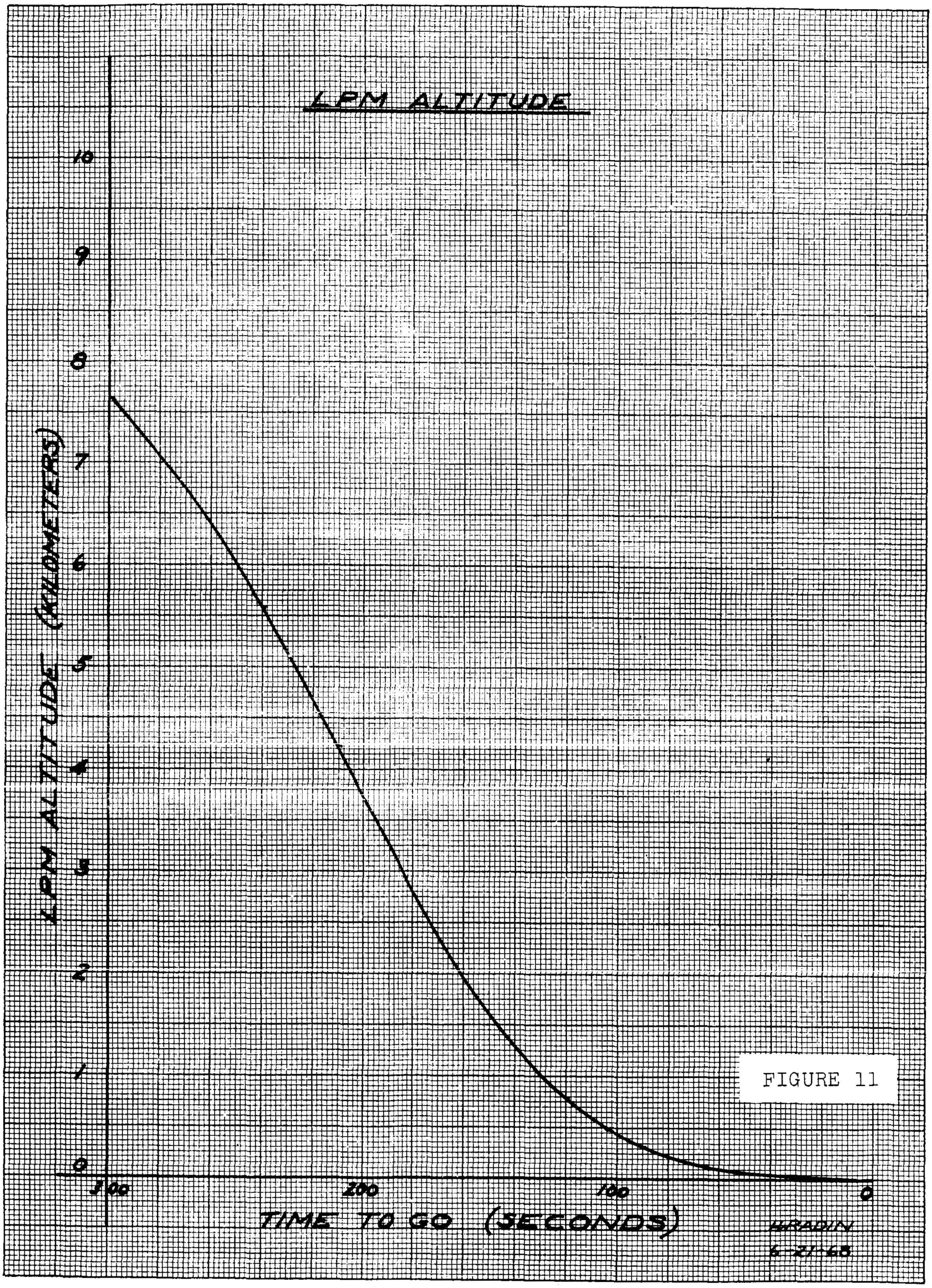
LPM ALTITUDE
LPM ALTITUDE (KILOMETERS)
10
9
8
7
6
5
4
3
2
1
0
300
200
100
0
TIME TO GO (SECONDS)
GRADIN
6-21-68

FIGURE 11

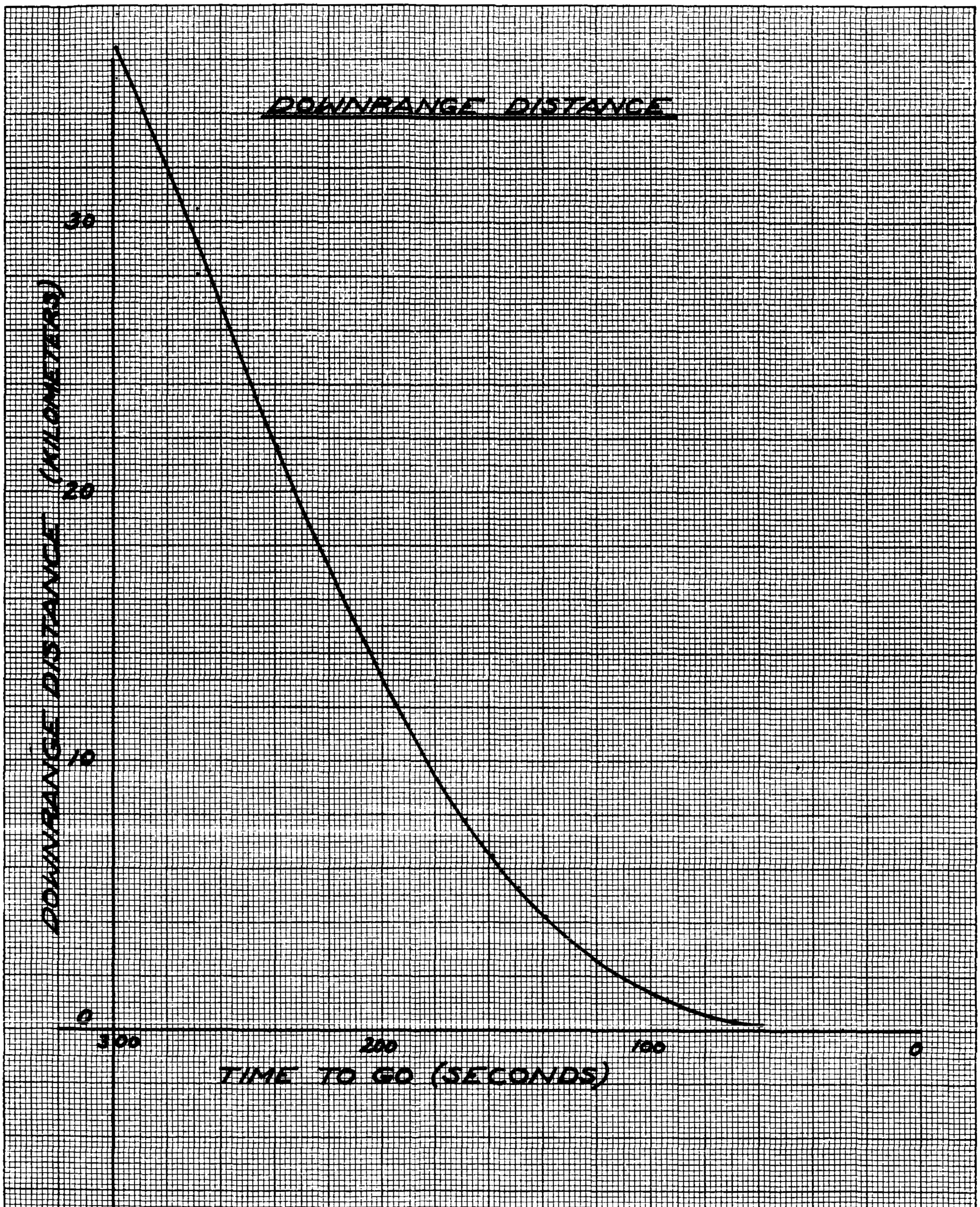
DOWNRANGE DISTANCE
DOWNRANGE DISTANCE (KILOMETERS)
30
20
10
0
-10
300
200
100
0
TIME TO GO (SECONDS)
W.RADIN
6-21-68

FIGURE 12

APPENDIX A

DERIVATION OF SEXTANT TRACKING RATE

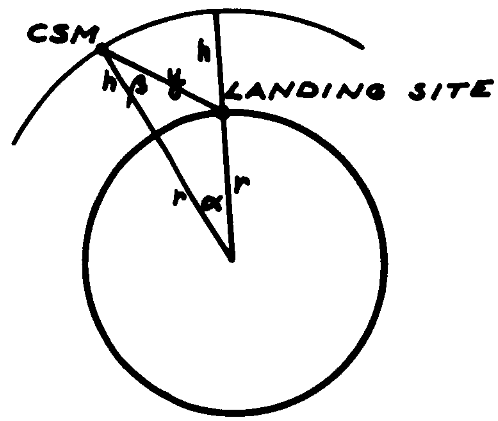

We should like to determine the rate of change of the angle β between the local vertical at the CSM and the landing site (we must of course add to this the angular rate of change of the local vertical as the CSM proceeds in its orbit). This angle β is the pointing angle of the CSM sextant, and $\frac{d\beta}{dt}$ is a measure of the difficulty of the tracking task.

From the law of cosines,

$$r^2 = (r + h)^2 + y^2 - 2y(r + h)\cos\beta \qquad \text{(A-1)}$$

which yields

$$\cos\beta = \frac{y^2 + h^2 + 2rh}{2y(r+h)} . \qquad \text{(A-2)}$$

Also,

$$y^2 = r^2 + (r + h)^2 - 2r(r + h)\cos\alpha \qquad \text{(A-3)}$$

Combining (A-1) and (A-3), we get

$$\cos\beta = \frac{1 - \delta \cos\alpha}{\sqrt{1 + \delta^2 - 2\delta \cos\alpha}}, \text{ where } \delta = \frac{r}{r + h}$$

$(-90° \leq \beta \leq 90°)$,

and $$\boxed{\cos^2\beta = \frac{(1 - \delta \cos\alpha)^2}{1 + \delta^2 - 2\delta \cos\alpha}} \tag{A-4}$$

Now $$\sin^2\beta = 1 - \cos^2\beta = \frac{\delta^2 \sin^2\alpha}{1 + \delta^2 - 2\delta \cos\alpha},$$

and $$\sin 2\beta = 2\sin\beta \cos\beta = \frac{2\delta \sin\alpha\ (1 - \delta \cos\alpha)}{1 + \delta^2 - 2\delta \cos\alpha}.$$

Differentiating (A-4),

$$d(\cos^2\beta) = -2 \sin\beta\cos\beta d\beta = -\sin 2\beta d\beta = d\left[\frac{(1 - \delta \cos\alpha)^2}{1 + \delta^2 - 2\delta \cos\alpha}\right]$$

Substituting for $\sin 2\beta$ on the left, and differentiating on the right, we obtain the result

$$\boxed{\frac{d\beta}{d\alpha} = \delta \frac{(\cos\alpha - \delta)}{1 + \delta^2 - 2\delta \cos\alpha}} \tag{A-5}$$

where we have chosen the positive root of $\sin^2\beta$ to assure that the algebraic signs of $\sin\alpha$ and $\sin\beta$ will be the same.

By the chain rule,

$$\boxed{\frac{d\beta}{dt} = \frac{\delta\ (\cos\alpha - \delta)}{1 + \delta^2 - 2\delta \cos\alpha} \cdot \frac{d\alpha}{dt}} \tag{A-6}$$

The period of an 80 nautical mile CSM orbit is slightly greater than two hours, and the angular velocity $\frac{d\alpha}{dt}$ is just

$$\frac{d\alpha}{dt} = -W_C = \frac{-360}{(122.77)(60)} = -0.048 \text{ degrees/second.}$$

For the same orbit,

$$\delta = \frac{r}{r + h} = \frac{\frac{1877}{2}}{\frac{1877}{2} + 80} = 0.9215.$$

Letting $\alpha = W_C T$, equation (A-6) may be written

$$\boxed{\frac{d\beta}{dt} = -\frac{\delta\ (\cos W_C T - \delta)}{1 + \delta^2 - 2\delta \cos W_C T} \cdot W_C} \text{ degrees/second} \tag{A-7}$$

Using the above numbers, equation (A-7) is plotted in Figure 2; T = 0 when the CSM is directly overhead at the landing site. The minus sign has been dropped in plotting the curve.

APPENDIX B

CALCULATION OF LORS/SEXTANT MEASUREMENT ERROR

We shall calculate the errors in the downrange and crossrange measurements independently, for the sake of simplicity, since our purpose is simply to show the usefulness of this technique. The CSM (or LPM) guidance computer will of course perform a vector addition in three dimensions.

Downrange Error

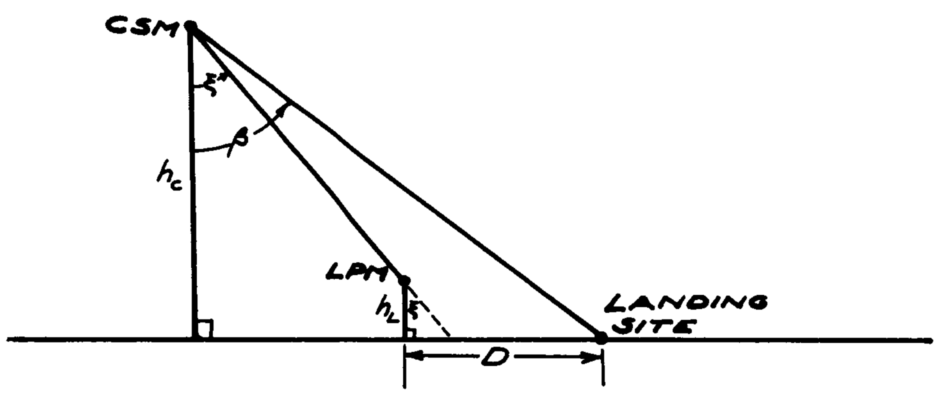

Assuming for the moment that the LPM has no crossrange error, and that it travels in the plane of this page, the expression for the downrange distance D of the LPM from the landing site is given by

$$D = h_L \tan\xi + h_C (\tan\beta - \tan\xi) \qquad \text{(B-1)}$$

The error in a measurement of D is given by the total differential,

$$\Delta D = \frac{\delta D}{\delta h_C} \Delta h_C + \frac{\delta D}{\delta h_L} \Delta h_L + \frac{\delta D}{\delta \beta} \Delta \beta + \frac{\delta D}{\delta \xi} \Delta \xi ; \qquad \text{(B-2)}$$

if the variables are independent, we must use instead ΔD_{rss}, where

$$\left(\Delta D_{rss}\right)^2 = \left(\frac{\delta D}{\delta h_C}\ \Delta h_C\right)^2 + \left(\frac{\delta D}{\delta h_L}\ \Delta h_L\right)^2 + \left(\frac{\delta D}{\delta \beta}\ \Delta \beta\right)^2 + \left(\frac{\delta D}{\delta \xi}\ \Delta \xi\right)^2 \qquad \text{(B-3)}$$

It can be shown that

$$\Delta D = (\tan\beta - \tan\xi)\ \Delta h_C + (\tan\xi)\ \Delta h_L - (h_C - h_L)(1 + \tan^2\xi)\ \Delta\xi + h_C(1 + \tan^2\beta)\ \Delta\beta \qquad \text{(B-4)}$$

and it follows directly that

$$\left(\Delta D_{rss}\right)^2 = (\tan\beta-\tan\xi)^2(\Delta h_C)^2+\tan^2\xi(\Delta h_L)^2+(h_C-h_L)^2(1+\tan^2\xi)^2(\Delta\xi)^2 +h_C{}^2(1+\tan^2\beta)^2(\Delta\beta)^2. \qquad \text{(B-5)}$$

The errors ΔD and ΔD_{rss} are plotted in Figures 4-6, and the individual components are plotted in Figures 7-9. For these curves, the values of h_C, h_L, β, and ξ have been obtained from a specific run of the BCMASP program, courtesy of F. Heap - this is a typical 80 nautical mile Apollo orbit and descent trajectory.

Various values for Δh_C, Δh_L, $\Delta\beta$, and $\Delta\xi$ were assumed, and noted on the curves; it was assumed that $\Delta h_C = \Delta h_L$ and $\Delta\beta = \Delta\xi$. The assumption of 0.0008 radians for $\Delta\beta$ and $\Delta\xi$ is discussed in Appendix C.

Crosstrack Error

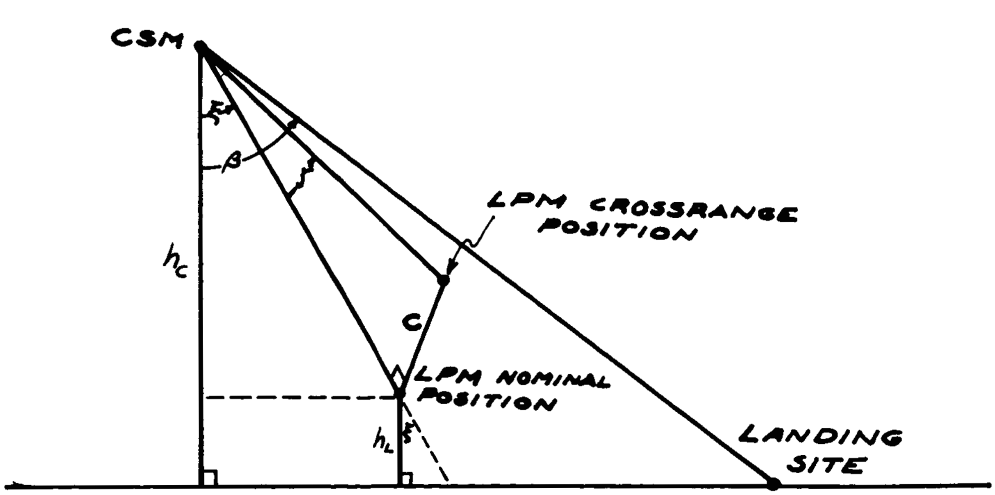

The crosstrack displacement (out of plane) may be obtained from

$$\frac{C}{\tan\zeta} = \frac{h_C - h_L}{\cos\xi} \text{ , or}$$

$$C = (h_C - h_L)\frac{\tan\zeta}{\cos\xi} \text{ .} \qquad \text{(B-6)}$$

As before,

$$\Delta C = \frac{\delta C}{\delta h_C}\Delta h_C + \frac{\delta C}{\delta h_L}\Delta h_L + \frac{\delta C}{\delta \xi}\Delta\xi + \frac{\delta C}{\delta\zeta}\Delta\zeta \qquad \text{(B-7)}$$

$$\Delta C = \frac{\tan\zeta}{\cos\xi}(\Delta h_C - \Delta h_L) + (h_C - h_L)\tan\zeta\frac{\tan\xi}{\cos\xi}\Delta\xi + \frac{h_C - h_L}{\cos\xi}\sec^2\zeta\Delta\zeta \qquad \text{(B-8)}$$

$$\left(\Delta C_{rss}\right)^2 = \frac{1}{\cos^2\xi}\left[\tan^2\zeta\,(\Delta h_C{}^2 + \Delta h_L{}^2) + (h_C - h_L)^2\tan^2\zeta\tan^2\xi(\Delta\xi)^2 + \frac{(h_C - h_L)^2}{\cos^4\zeta}(\Delta\zeta)^2\right] \qquad \text{(B-9)}$$

Since the angle errors are the same in all directions, $(\Delta\xi)^2 \equiv (\Delta\zeta)^2$; also, $\cos^4\zeta \doteq 1 - 2\zeta^2$ and $\tan^2\zeta \doteq \zeta^2$ for $\zeta<<1$. Then

$$\left(\Delta C_{rss}\right)^2 \doteq \frac{1}{\cos^2\xi}\left[(\Delta h_C{}^2 + \Delta h_L{}^2)\,\zeta^2 + (h_C - h_L)^2\zeta^2\tan^2\xi(\Delta\xi)^2 + \frac{(h_C - h_L)^2}{1 - 2\zeta^2}(\Delta\xi)^2\right] \qquad \text{(B-10)}$$

Now letting $\frac{1}{1 - 2\zeta^2} \doteq 1 + 2\zeta^2$, and collecting terms,

$$\left(\Delta C_{rss}\right)^2 \doteq \frac{1}{\cos^2\xi}\left[(\Delta h_C{}^2 + \Delta h_L{}^2)\ \zeta^2 + (h_C - h_L)^2(\Delta\xi)^2\left[1 + \zeta^2(2 + \tan^2\xi)\right]\right] \tag{B-11}$$

As an example, consider the case

$\Delta h_C = \Delta h_L = 2$ km

$\Delta\xi = \Delta\zeta = 0.0008$ radians

$\xi = 45°$

$h_C = 148$ km

$h_L \doteq 7$ km

from the Apollo trajectory, and assume an actual crosstrack displacement of C = 2.5 km. Then

$$\zeta = \tan^{-1}\left[\frac{C\ \cos\xi}{h_C - h_L}\right] = \tan^{-1}\frac{(1)\left(\frac{1.414}{2}\right)}{141} \doteq \tan^{-1}(0{,}0125) \doteq 0{,}0125 \text{ rad,}$$

This gives

$$\left(\Delta C_{rss}\right)^2 \doteq 2\left[(2^2 + 2^2)(0.0125)^2 + (141)^2(0.0008)^2\left[1 + (0.0125)^2(2 + 1)\right]\right]$$

$$\doteq 2\left[(8)(0.0125)^2 + (141)^2(0.0008)^2\right]$$

$$\doteq 2\ (1.40)\ 10^{-2}\ \mathrm{km}^2$$

and

$$\boxed{\Delta C_{rss} \doteq 167 \text{ meters}}$$

An examination of the numbers allows us to assume

$$\zeta^2(2 + \tan^2\xi) \ll 1$$

for any reasonable values of the variables. Then

$$\boxed{\left(\Delta C_{rss}\right)^2 \doteq \frac{1}{\cos^2\xi}\left[(\Delta h_C{}^2 + \Delta h_L{}^2)\ \zeta^2 + (h_C - h_L)^2\ (\Delta\xi)^2\right]} \quad . \quad \text{(B-12)}$$

Figure 10 is a plot of ΔC_{rss} as a function of T_{GO} for the three height error values assumed for the downrange case; the curves also assume that the initial value of C is 2.5 km, the 3σ uncorrected crossrange error of the LPM.

APPENDIX C

The assumption of 0.0008 radians (0.8 mr) for $\Delta\beta$ and $\Delta\xi$ is obtained as follows:

For the CSM, an initial 3-axis (1σ) misalignment of 114 arc seconds (0.553 mr), combined (rss) with 70 minutes of drift at 0.5 mr/hr (coasting).

For the LM, an initial misalignment of 0.553 mr combined with 60 minutes of drift at 0.5 mr/hr and 10 minutes of drift at 1.75 mr/hr (powered flight).

Each of these rss additions results in a total IMU error of 0.0008 radians, 1σ.